EPR study of light-induced regulation of photosynthetic electron transport in *Synechocystis* sp. strain PCC 6803

Boris V. Trubitsin[a], Mahir D. Mamedov[b], Liya A. Vitukhnovskaya[b], Alexey Yu. Semenov[b,*], Alexander N. Tikhonov[a,**]

[a] *Department of Biophysics, Faculty of Physics, M.V. Lomonosov Moscow State University, Moscow 119899, Russia*
[b] *A.N. Belozersky Institute of Physico-Chemical Biology, M.V. Lomonosov Moscow State University, Moscow 119899, Russia*

Received 28 February 2003; accepted 7 April 2003

First published online 8 May 2003

Edited by Richard Cogdell

Abstract The kinetics of the light-induced redox changes of the photosystem 1 (PS 1) primary donor P_{700} in whole cells of the cyanobacteria *Synechocystis* sp. PCC 6803 were studied by the electron paramagnetic resonance method. It was shown that the linear photosynthetic electron transport in cyanobacteria was controlled by two main mechanisms: (i) oxygen-dependent acceleration of electron transfer from PS 1 to $NADP^+$ due to activation of the Calvin cycle reactions and (ii) retardation of electron flow between two photosystems governed by a transmembrane proton gradient. In addition to the linear photosynthetic electron transport, cyanobacteria were capable of maintaining alternative pathways involving cyclic electron transfer around PS 1 and respiratory chains.

Key words: Electron transport in *Synechocystis* sp. PCC 6803; Photosynthetic control; Effect of oxygen

1. Introduction

Our knowledge of the primary photosynthetic processes has been mainly obtained from studies of isolated thylakoids or solubilized membrane complexes. However, the isolation procedure may impair both physiological function and regulation. For in vivo studies, the functional analysis of unicellular cyanobacteria is an easier task than that of plants. Cyanobacteria contain both oxygenic photosynthetic and respiratory electron transfer chains incorporated in the same membrane. The cyanobacterium *Synechocystis* sp. PCC 6803 is the first photosynthetic organism with a completely sequenced genome [1]. The X-ray crystal structures of the photosystem 1 (PS 1) and PS 2 complexes were recently resolved in closely related cyanobacterium *Synechococcus elongatus* [2,3].

The main biophysical techniques applied to in vivo studies of the photosynthetic electron transfer and related processes include: optical absorption spectroscopy, kinetic analysis of the fluorescent yields of chlorophyll and indicator dyes, and electron paramagnetic resonance (EPR) spectroscopy (see for review [4–8]). The EPR method has the obvious advantages for non-invasive monitoring the light-induced redox transients of the PS 1 primary donor P_{700}: (i) in contrast to optical spectroscopy methods, the EPR method allows to avoid possible artifacts due to side effects of monitoring and actinic light beams; (ii) high optical density of sample does not limit the registration of the EPR signal from the photooxidized centers P_{700}^+ in native systems.

In this work, in order to elucidate the factors of regulation of electron transport in *Synechocystis* sp. PCC 6803 cells, we studied the influence of oxygen and the effects of cofactors and inhibitors of electron transport on the kinetics of light-induced redox transients of the PS 1 primary donor P_{700}.

2. Materials and methods

Wild-type *Synechocystis* sp. PCC strain 6803 cells were grown in BG-11 medium [9]. Liquid cultures (ca. 8 l) were grown at 30°C under constant cool white fluorescent illumination (100 μE m^{-2} s^{-1}); air without supplemented CO_2 was bubbled through the cultures. Cell growth was monitored by measuring absorbance at 730 nm using a Shimadzu UV-1601 spectrophotometer. Cells from liquid cultures in the late exponential phase of growth (A_{730} = 1–1.2) were harvested by centrifugation and washed once with 50 mM HEPES-NaOH buffer, pH 7.5. Cells were stored at −75°C with 20% (v/v) glycerol at a chlorophyll concentration of 1 mg ml^{-1}.

The EPR spectra were measured with a Varian E-4 X-band spectrometer. Samples were placed either in an oxygen-permeable plastic tube [10] or standard flat quartz cuvette positioned in the resonator of the EPR spectrometer. Cells were illuminated with a subsaturating white light from a 100-W tungsten lamp; infrared light was cut off with a 5-cm layer of water. Continuous illumination (∼1 mE m^{-2} s^{-1} on the surface of a sample) was switched off with a mechanical shutter (actuation time < 1 ms). The EPR spectra were recorded at 23°C at subsaturating microwave power 10 mW and modulation amplitude 4 G.

3. Results and discussion

3.1. Kinetics of light-induced oxidation of P_{700} and the effects of oxygen deprivation

Fig. 1 demonstrates typical patterns of the light-induced changes in the height of the EPR signal from oxidized reaction centers P_{700}^+ in *Synechocystis* sp. PCC 6803. Suspension of cyanobacteria cells was placed either in an oxygen-permeable tube (Fig. 1A) or in an oxygen-impermeable quartz cell (Fig. 1B). Illumination of cells with white light initiated the appearance of the EPR signal characterized by the linewidth ΔH_{pp} = 8 G and g = 2.0025 (Fig. 1C). This signal was typical

*Corresponding author. Fax: (7)-095-9393181.
**Also corresponding author.
E-mail addresses: semenov@genebee.msu.su (A.Y. Semenov), an_tikhonov@newmail.ru (A.N. Tikhonov).

0014-5793/03/$22.00
doi:10.1016/S0014-5793(03)00429-0

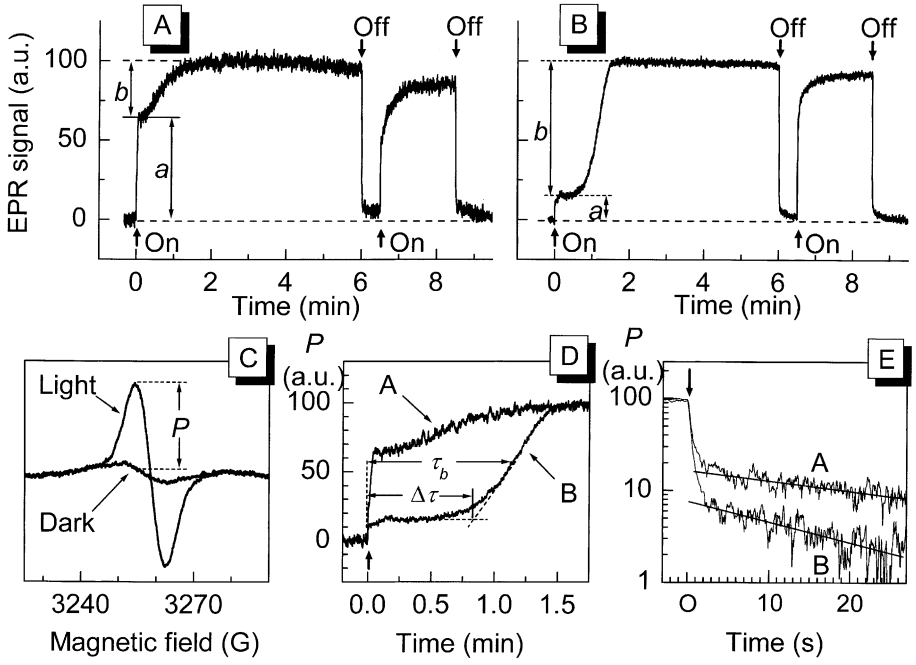

Fig. 1. Light-induced changes in the EPR signal in cyanobacteria. Kinetics of the signal amplitude *P* changes were measured for cells placed either in an oxygen-permeable plastic tube (A) or a quartz cuvette (B). C: EPR spectra recorded in the dark and during the illumination of cells. D: Extended kinetics of the signal rise in response to switching on the light. E: Extended kinetics of the signal decay after ceasing the illumination. The concentration of photochemically active reaction centers P_{700} determined from the intensity of the EPR signal was equal to 10 μM. Incubation medium contained 50 mM HEPES (pH 7.5) and 20% glycerol.

of the EPR signal from P_{700}^{+} [11][1]. For monitoring the kinetics of the light-induced changes in the height of this signal, the magnetic field was fixed at the low-field extreme of the signal. In order to standardize the state of cells before kinetic measurements, each sample was preliminary illuminated for 1 min with white light and then adapted to the dark for 10 min. Similarly to intact chloroplasts of higher plants in situ, the kinetics of the light-induced oxidation of P_{700} depended on the prehistory of illumination, i.e. dark adaptation time [12,13] and the presence of oxygen in the cell suspension.

For cells placed in a gas-permeable tube (Fig. 1A), we observed two distinct kinetic phases of P_{700} oxidation induced by continuous illumination (phases *a* and *b*). A relatively fast initial phase *a* (ca. 60–65% of the total signal), was followed by a certain lag period ($\Delta\tau \approx 10$ s) and after that, by a rather slow ($\tau_b \approx 40$ s) increase in the signal amplitude (phase *b*, ca. 35–40%) to a steady-state level (see Fig. 1D for definitions of the kinetic parameters τ_b and $\Delta\tau$). The ratio between the amplitudes of phases *a* and *b* was virtually independent of the dark adaptation, whereas the kinetic parameter τ_b characterizing the light-induced rise of the signal shortened with the decrease in the adaptation time. After ceasing the illumination, the EPR signal decayed to the initial level. The kinetics of P_{700}^{+} dark reduction (Fig. 1E) were characterized by the fast ($t_{1/2} \approx 0.05$ s) and the slow ($t_{1/2} \approx 15$–25 s) components. The contribution of the fast component dominated (ca. 83–90%) over the slow one (ca. 10–17%).

In case of dark-adapted cells in an oxygen-impermeable quartz cuvette, we observed a different pattern of the light-induced redox transients of P_{700} (Fig. 1B). The amplitude of the initial rise of the EPR signal (phase *a*) was substantially smaller (ca. 15%) than the amplitude of the second phase *b* (ca. 85%). After sufficiently long (>2 min) dark adaptation, we observed an extended lag phase ($\Delta\tau \approx 50$ s) that preceded the signal rise to a steady-state level ($\tau_b \approx 70$ s). Contrary to cells placed in a gas-permeable tube, the ratio of the amplitudes of phases *a* and *b* strongly depended on the dark adaptation time. Fig. 1B demonstrates that after a relatively short dark adaptation (30 s), the amplitude of the fast phase *a* significantly increased at the expense of the slower phase *b*. The reduction of P_{700}^{+} after switching the illumination off followed two-exponential kinetics (Fig. 1E). The contribution of the slow component ($\tau_{1/2} \approx 15$ s) was negligible (ca. 8%).

There are good reasons to believe that the difference between the kinetic patterns presented in Fig. 1A,B was caused by oxygen deprivation inside the quartz cuvette during the dark adaptation of cells[2]. The consumption of oxygen could occur due to the functioning of terminal oxidases found in both thylakoid and cytoplasmic membranes of *Synechocystis* 6803 (see [15,16] for review). The results of experiments presented in Fig. 2 clearly demonstrated that the limitation of electron efflux from the acceptor side of PS 1 caused by oxy-

[1] Additional argument in favor of P_{700}^{+} as a source of this EPR signal comes from similarity between the kinetics of the light-induced changes in the EPR signal and in the absorption changes observed in a suspension of cyanobacteria cells at 703 nm (not shown).

[2] This conclusion has been supported by the results of our measurements of oxygen concentration in a suspension of cyanobacteria cells with the oxygen-sensitive spin probe CTPO (3-carbamoyl-2,2,5,5-tetramethyl-3-pyrroline-1-yloxyl [14]). We found that after 2–4 min of dark adaptation the oxygen concentration in a cell suspension in a quartz cuvette decreased by a factor of 3–4, whereas the concentration of oxygen inside a gas-permeable tube did not decrease (to be published elsewhere).

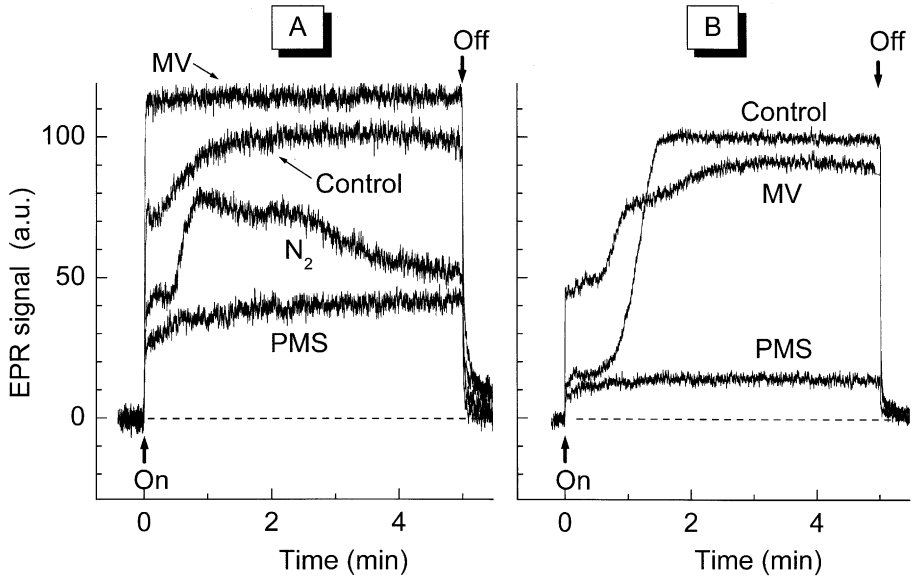

Fig. 2. Effects of MV, PMS and nitrogen blowing (10 min) on the light-induced changes in the intensity of the EPR signal. A: Cells in an oxygen-permeable plastic tube; B: cells in a quartz cuvette. Cells were incubated in the presence of 100 μM MV for 40 min before the EPR measurements. Concentration of PMS – 50 μM. Cell concentration and incubation medium were as in Fig. 1.

gen deficit was one of the main reasons for a relatively low level of oxidized centers P_{700}^{+} on the initial stage of illumination (phase *a*) of dark-adapted cells in a quartz cuvette. The subsequent rise of the EPR signal from P_{700}^{+} (phase *b*) is likely to be associated with the light-induced regeneration of oxygen by the water splitting complex of PS 2. Note that the adaptation-dependent effect described above cannot be explained by the trivial disappearance of $NADP^{+}$ or CO_2 depletion. Actually, we observed retardation of the light-induced oxidation of P_{700} after dark adaptation of cells in a quartz cuvette (Fig. 1B), when O_2 (but not CO_2) was consumed by the respiratory chains. Meanwhile, illumination of dark-adapted cells for a rather long period (up to 6 min), when CO_2 molecules could be consumed (and therefore the NADPH/$NADP^{+}$ ratio should be increased), did not cause the decrease in the steady-state level of P_{700}^{+} (Fig. 1B).

The level of the EPR signal, as well as its kinetic characteristics, can be modulated by replacement of oxygen with gaseous nitrogen (Fig. 2A). Similarly to dark-adapted cells in a quartz cuvette (Fig. 2B), blowing a plastic tube with nitrogen was found to cause a decrease in the amplitude of phase *a* and the appearance of a distinct lag phase followed by the signal rise (Fig. 2A). After a maximal level had been reached, the concentration of oxidized centers P_{700}^{+} gradually decreased. The effect of nitrogen treatment was reversible: further aeration of the sample resulted in recovery of the initial kinetic pattern (not shown). In contrast to the effect caused by blowing with N_2, the addition of methyl viologen (MV), an artificial electron acceptor of PS 1, stimulated the light-induced oxidation of P_{700}. In aerated cells (Fig. 2A) in the presence of 0.1 mM MV, the amplitude of the fast phase *a* markedly increased at the expense of the slow phase *b*. In cells adapted to the dark in a quartz cuvette (Fig. 2B), the addition of MV also induced a pronounced increase in the phase *a* amplitude at the expense of the slower phase *b*. The remaining slow phase *b* of the EPR signal rise could be explained by oxygen deficiency that prevents reoxidation of MV and/or by insufficient concentration of MV inside cells due to poor permeability of cell membranes to MV. Results of experiments presented in Fig. 2 support the notion that the oxygen-dependent efflux of electrons from PS 1 controls the rate of photosynthetic electron transfer in cyanobacteria.

If the efflux of electrons from PS 1 is restricted, the linear (non-cyclic) electron flow might switch to a cyclic pathway around PS 1 (for review see [17,18]). We suggested that in oxygen-deficient cells cyclic electron transport could sustain the ATP synthesis, providing thereby the functioning of the Calvin cycle. Cyclic electron transport can be simulated by the addition of phenazine methosulfate (PMS), an artificial mediator of cyclic electron transport. In the presence of PMS, the phase *a* amplitude decreased, compared to control samples, in both aerated (Fig. 2A) and oxygen-deficient (Fig. 2B) samples. In the two cases, the appearance of phase *b* was reduced by PMS. Less efficient action of PMS in an aerated suspension of cells (Fig. 2A), compared to oxygen-deficient cells (Fig. 2B), can be explained by the competition between PMS and oxygen for electrons on the acceptor side of PS 1. The effect of PMS was also observed in the presence of 3-(3,4-dichlorophenyl)-1,1-dimethylurea (DCMU), an inhibitor of PS 2 (data not shown), demonstrating that PMS mediated a cyclic electron transport around PS 1.

3.2. *Effects of electron transport inhibitors on the light-induced redox transients of P_{700}*

3.2.1. KCN. The effect of KCN on the light-induced redox transients of P_{700} strongly depended on experimental conditions. In aerated samples (Fig. 3A), the addition of KCN facilitated the oxidation of P_{700}. In the presence of KCN, we observed only the fast phase *a*. Its amplitude was substantially higher than the amplitude of the total signal (phase *a* plus phase *b*) in control samples. It is noteworthy that in the KCN-inhibited cells, the rate of P_{700}^{+} decay after switching off the illumination slowed down dramatically (Fig. 3A,C). The contribution of the slow component ($t_{1/2} \approx 15$ s) gradually increased with the concentration of KCN. This component accounted for about 70% of the signal decay at 8 mM

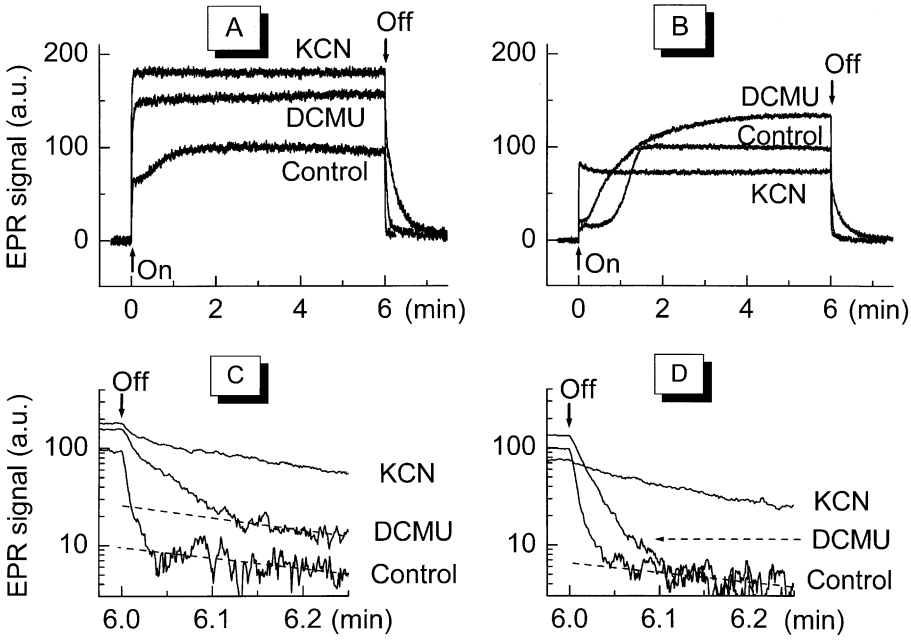

Fig. 3. Effects of KCN and DCMU on the light-induced changes in the intensity of the EPR signal. A, C: Cells in an oxygen-permeable plastic tube; B, D: cells in a quartz cuvette. C and D: Extended decay kinetics of the EPR signal corresponding to (A) and (B), respectively. Concentration of KCN – 8 mM, DCMU – 0.1 mM. Cell concentration and incubation medium were as in Fig. 1.

KCN (Fig. 3C). The fast decay component was completely suppressed at higher concentrations (data not shown). The inhibitory effect of KCN can be explained by the influence of KCN on plastocyanin (Pc) [19] and/or cytochrome c_6 (cyt c_6) [20], which serve as the immediate electron donors to P^+_{700} in cyanobacteria.

If cells were incubated in an oxygen-impermeable quartz cuvette (Fig. 3B), the addition of KCN promoted the increase in the amplitude of the fast phase *a*, whereas the slow phase *b* was completely inhibited. Note that the steady-state level of the signal was lower than in control sample. Similarly to cells placed in a plastic tube, the addition of KCN dramatically slowed down the kinetics of P^+_{700} decay after switching off illumination (Fig. 3B). The two effects, i.e. stimulation of P_{700} oxidation and slowing down the signal decay, can be attributed to the effect of KCN on the donor side of PS 1. The elimination of phase *b* by KCN in dark-adapted cells in a quartz cuvette (Fig. 3B) indicates the retardation of electron efflux from PS 1. This effect of KCN can be explained by two reasons: (i) inhibition of $NADP^+$ recovery in the Calvin cycle [21], and (ii) inhibition of NADPH oxidation by the respiratory chain. Actually, under conditions of oxygen deficiency, $NADP^+$ is the only terminal electron acceptor for PS 1. Therefore, if the utilization of NADPH is inhibited by KCN, the low rate of electron efflux from PS 1 should limit the light-induced oxidation of P_{700}. Another possible reason for restriction of electron flow by KCN is the inhibition of catalase, which provides regeneration of oxygen in a cell suspension to support pseudo-cyclic electron transport [22].

Comparison of the KCN effects in aerated and oxygen-deficient cells leads to the following conclusions: (a) in the presence of oxygen, inhibition of the Calvin cycle reactions by KCN does not preclude the efflux of electrons from PS 1; (b) in oxygen-deficient cell suspension, electron transfer to the terminal electron acceptor ($NADP^+$) can be the rate-limiting step of the linear electron transport chain.

3.2.2. DCMU. In the presence of DCMU, both in aerated (Fig. 3A) and in oxygen-depleted cell suspensions (Fig. 3B), we observed an increase in the steady-state levels of P^+_{700} compared to relevant control samples. This effect can be explained, in general, by decreasing the electron flow to P^+_{700} from PS 2. During the illumination of aerated suspension (Fig. 3A), the EPR signal rapidly reached the steady-state level, while the slow phase *b* was completely inhibited. The effect of DCMU on the signal amplitude was somewhat lower than that of KCN. The rate of P^+_{700} reduction after switching the illumination off (Fig. 3C) was substantially slower ($t_{1/2} \approx 2.5$–3 s) than in control sample ($t_{1/2} \approx 0.05$ s), but faster than in KCN-treated cells ($t_{1/2} \approx 15$ s).

For cells adapted to the dark in a quartz cuvette, in the presence of DCMU we observed two-phase kinetics of the light-induced oxidation of P_{700} (Fig. 3B). The amplitude of phase *a* was almost the same as in control cells, whereas the amplitude of phase *b* was markedly higher. In DCMU-treated cells we also observed a short but distinct lag period that preceded the signal rise (phase *b*). It should be noted that in oxygen-deficient cells, the rate of P^+_{700} reduction after switching the illumination off was faster ($t_{1/2} \approx 1$ s, Fig. 3D) than in aerated sample ($t_{1/2} \approx 2.5$–3 s, Fig. 3C). This result can be explained by oxygen-controlled redistribution of electron fluxes between photosynthetic and respiratory chains. In an aerated suspension of cells, the terminal oxidases compete with P^+_{700} for electrons from plastoquinol ($PQH_2 \rightarrow$ cyt $bd \rightarrow O_2$) and cyt c_6 (cyt $c_6 \rightarrow$ cyt $aa_3 \rightarrow O_2$) pools, thus decreasing the contribution of a fast component of P^+_{700} reduction ($PQH_2 \rightarrow bf \rightarrow$ Pc/cyt $c_6 \rightarrow P^+_{700}$).

Taking all of these findings into account, we assume that in the presence of DCMU cyanobacteria retain the electron flow to P^+_{700} associated with cyclic electron transfer around PS 1, as well as the functioning of respiratory electron transport chains donating electrons to the plastoquinone pool, e.g. through the NAD(P)H-dehydrogenase (NDH-1) complex (NADPH →

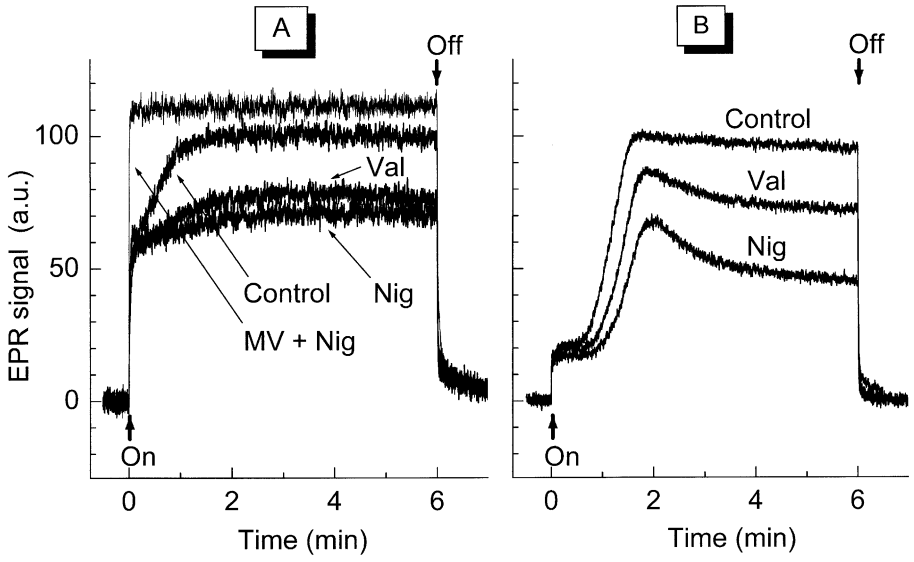

Fig. 4. Effects of valinomycin and nigericin on the light-induced changes in the intensity of the EPR signal. A: Cells in an oxygen-permeable plastic tube; B: cells in a quartz cuvette. 100 μM valinomycin or 100 μM nigericin in the presence of 30 mM KCl were added as indicated. The upper trace on Fig. 4A corresponds to the addition of MV (100 μM) in the presence of 100 μM nigericin. Cell concentration and incubation medium were as in Fig. 1.

NDH-1 → PQ → *bf* → Pc/cyt c_6 → P_{700}^+). According to [15,16], the electron transfer capacities of oxidases were shown to be about 10% relative to photosynthetic electron transfer.

3.3. Uncouplers

For aerated cells (Fig. 4A), the addition of nigericin or valinomycin caused a decrease in the steady-state level of P_{700}^+ at the expense of phase *b*, whereas the amplitude of the initial phase *a* was not affected. It is noteworthy that the effect of nigericin was more pronounced than that of valinomycin. This result means that the transmembrane pH difference (ΔpH) rather than the transmembrane electric potential difference ($\Delta\psi$) is a dominant factor that influences photosynthetic electron transport in cyanobacteria.

We suppose that a relatively slow oxidation of P_{700} during the phase *b* was caused mainly by acceleration of electron efflux from PS 1 to $NADP^+$ due to the light-induced activation of the Calvin cycle reactions. This could occur due to: (i) $\Delta\mu_{H^+}$-dependent activation of ATP synthase [23], and (ii) thioredoxin-mediated activation of the Calvin cycle enzymes [24]. Actually, in the presence of MV the EPR signal of P_{700}^+ rapidly reached a steady-state level, which was higher than that in the control sample (Fig. 2A). Suppression of phase *b* by uncouplers (Fig. 4A) can be explained by inhibition of ATP synthesis that is necessary for the NADPH recycling in the Calvin cycle. It is notable that the addition of MV stimulated the oxidation of P_{700} not only in the absence but also in the presence of nigericin (Fig. 4A).

We also suppose that the feedback control of electron transport between two photosystems governed by $\Delta\mu_{H^+}$ can contribute to a relatively slow oxidation of P_{700} (phase *b*). The suppression of phase *b* by uncouplers (Fig. 4A) could be explained, at least partially, by the release of the photosynthetic control. In higher plant chloroplasts, the ΔpH-dependent decrease in the electron flow rate between two photosystems was revealed as slowing down of P_{700}^+ reduction after sudden switching the illumination off [4,12,25,26]. In chloroplasts, we observed that the addition of nigericin decreased the characteristic time of dark reduction of P_{700}^+ by approximately one-half (data not shown). This result substantiated the suggestion that in cyanobacteria the rate of electron transport between two photosystems was also controlled by ΔpH.

The effects of uncouplers under the oxygen-deficiency conditions were more pronounced than in aerated samples (Fig. 4B). The substantial decrease in the steady-state levels of the signal can be explained by acceleration of oxygen depletion in a quartz cuvette due to the release of the photosynthetic and respiratory control.

4. Concluding remarks

The EPR study of the light-induced redox transients of the P_{700} has demonstrated that photosynthetic electron transport in *Synechocystis* sp. PCC 6803 is controlled both at the donor and at the acceptor sides of PS 1. The light-induced energization of thylakoid membranes leads to stimulation of electron efflux from PS 1 to $NADPH^+$, which is most probably due to activation of the Calvin cycle reactions, and causes the retardation of electron transport between two photosystems governed by $\Delta\mu_{H^+}$. The efficiency of linear electron transport strongly depends on the presence of oxygen in cell suspension: under oxygen-deficient conditions, the efflux of electrons from PS 1 becomes the rate-limiting step. In line with the data obtained in [27,28], we conclude that under certain conditions (oxygen deficiency, inhibition of PS 2), cyanobacteria retain photosynthetic electron transport associated with cyclic electron flow around PS 1 and reduction of the plastoquinone pool by the respiratory electron transport chains.

Acknowledgements: The authors thank Dr. I. Elanskaya for the gift of cyanobacteria cells and Dr. S. Chamorovsky for critical reading of the manuscript. This work was supported by Grants 99-1086 (to A.N.T.) and 01-483 (to A.Y.S. and A.N.T) from the INTAS, Grants from the Russian Foundation for Basic Research 03-04-48983 (to A.Y.S.), 03-04-48981 (to A.N.T.) and 01-04-49268 (to M.D.M.), Grant from the International Science and Technology Center (ISTC) 2296, and Grant for biophotonics research from Moscow State University.

References

[1] Kaneko, T., Sato, S., Kotani, A., Tanaka, A., Asamizu, E., Nakamura, Y., Miyajima, N., Hirosawa, M., Sugiura, M., Sasamoto, S., Kimura, T., Hosochi, T., Matsuno, A., Muraki, A., Nakazaki, N., Naruo, K., Okamura, S., Shimpo, S., Takenchi, C., Wada, T., Watanabe, A., Yamada, M., Yasuda, M. and Tabata, S. (1996) DNA Res. 3, 109–136.

[2] Zouni, A., Witt, H.T., Kern, J., Fromme, P., Krauss, N., Saenger, W. and Orth, P. (2001) Nature 409, 739–743.

[3] Jordan, P., Fromme, P., Witt, H.T., Klukas, O., Saenger, W. and Krauss, N. (2001) Nature 411, 909–917.

[4] Blumenfeld, L.A. and Tikhonov, A.N. (1994) Biophysical Thermodynamics of Intracellular Processes, Molecular Machines of the Living Cell, Springer-Verlag, New York.

[5] Amesz, J. and Hoff, A.J. (1996) in: Biophysical Techniques in Photosynthesis, Part two: Magnetic Resonance, pp. 209–313, Kluwer, Dordrecht.

[6] Joliot, P., Beal, D. and Delosme, R. (1998) in: The Molecular Biology of Chloroplasts and Mitochondria in *Chlamydomonas* (Rochaix, J.-D., Goldschmidt-Clermon, M. and Merchant, S., Eds.), pp. 433–449, Kluwer, Dordrecht.

[7] Lazar, D. (1999) Biochim. Biophys. Acta 1412, 1–28.

[8] Teuber, M., Rogner, M. and Berry, S. (2001) Biochim. Biophys. Acta 1506, 31–46.

[9] Rippka, R., Derulles, J., Waterbury, J.B., Herdman, M. and Stanier, R.Y. (1979) J. Gen. Microbiol. 181, 1–60.

[10] Hyde, J.S. and Subczynski, W.K. (1989) in: Biological Magnetic Resonance. Spin Labeling. Theory and Applications (Berliner, L.J. and Rueben, J., Eds), Vol. 8, pp. 399–425, Plenum Press, New York.

[11] Webber, A.N. and Lubitz, W. (2001) Biochim. Biophys. Acta 1507, 61–79.

[12] Tikhonov, A.N., Khomutov, G.B., Ruuge, E.K. and Blumenfeld, L.A. (1981) Biochim. Biophys. Acta 637, 321–333.

[13] Andreeva, A.S. and Tikhonov, A.N. (1983) Photobiochem. Photobiophys. 6, 261–266.

[14] Subczynski, W.K., Cieslikowska, A. and Tikhonov, A.N. (1990) Photosynthetica 24, 75–84.

[15] Peschek, G.A. (1987) in: *The Cyanobacteria* (Fay, P. and Van Baalen, C., Eds.), pp. 119–161, Elsevier, Amsterdam.

[16] Schmetterer, G. (1994) in: The Molecular Biology of Cyanobacteria (Bryant, D.G., Ed.), pp. 409–435, Kluwer, Dordrecht.

[17] Bendall, D.S. and Manasse, R.S. (1995) Biochim. Biophys. Acta 1229, 23–38.

[18] Joliot, P. and Joliot, A. (2002) Proc. Natl. Acad. Sci. USA 99, 10209–10214.

[19] Izawa, S. (1977) in: Photosynthesis I (Trebst, A. and Avron, M., Eds.), pp. 266–282, Springer-Verlag, Berlin.

[20] Schejter, A. and George, P. (1965) Nature 206, 1150–1154.

[21] Ishida, H., Shimizu, S., Makino, A. and Mae, T. (1998) Planta 204, 305–309.

[22] Backhausen, J.E., Kitzmann, C., Horton, P. and Scheibe, R. (2000) Photosynth. Res. 64, 1–13.

[23] Evron, Y., Johnson, E.A. and McCarty, R.E. (2000) J. Bioenerg. Biomembr. 32, 501–506.

[24] Buchanan, B.B. (1980) Annu. Rev. Plant Physiol. Plant Mol. Biol. 31, 341–374.

[25] Rumberg, B. and Siggel, U. (1969) Naturwissenschaften 56, 130–132.

[26] Kramer, D.M., Sacksteder, C.A. and Cruz, J.A. (1999) Photosynth. Res. 60, 151–163.

[27] Howitt, C.A., Cooley, J.W., Wiskich, J.T. and Vermaas, W.F.J. (2001) Planta 214, 46–56.

[28] Berry, S., Schneider, D., Vermaas, W.F.J. and Rogner, M. (2002) Biochemistry 41, 3422–3429.